



Observation of $B^+ \rightarrow \Lambda\bar{\Lambda}K^+$

Y.-J. Lee,²⁴ M.-Z. Wang,²⁴ K. Abe,⁷ K. Abe,³⁹ T. Abe,⁷ H. Aihara,⁴¹ Y. Asano,⁴⁵ V. Aulchenko,¹ T. Aushev,¹¹ T. Aziz,³⁷ S. Bahinipati,⁴ A. M. Bakich,³⁶ Y. Ban,³¹ I. Bedny,¹ U. Bitenc,¹² I. Bizjak,¹² A. Bondar,¹ A. Bozek,²⁵ M. Bračko,^{18, 12} J. Brodzicka,²⁵ T. E. Browder,⁶ P. Chang,²⁴ Y. Chao,²⁴ B. G. Cheon,³ R. Chistov,¹¹ S.-K. Choi,⁵ Y. Choi,³⁵ A. Chuvikov,³² M. Danilov,¹¹ M. Dash,⁴⁶ L. Y. Dong,⁹ A. Drutskoy,⁴ S. Eidelman,¹ V. Eiges,¹¹ S. Fratina,¹² N. Gabyshev,¹ A. Garmash,³² T. Gershon,⁷ G. Gokhroo,³⁷ B. Golob,^{17, 12} R. Guo,²² J. Haba,⁷ K. Hayasaka,²⁰ H. Hayashii,²¹ M. Hazumi,⁷ T. Higuchi,⁷ L. Hinz,¹⁶ T. Hokuue,²⁰ Y. Hoshi,³⁹ W.-S. Hou,²⁴ Y. B. Hsiung,^{24, *} A. Imoto,²¹ K. Inami,²⁰ A. Ishikawa,⁷ R. Itoh,⁷ H. Iwasaki,⁷ M. Iwasaki,⁴¹ J. H. Kang,⁴⁷ J. S. Kang,¹⁴ N. Katayama,⁷ H. Kawai,² T. Kawasaki,²⁷ H. R. Khan,⁴² H. Kichimi,⁷ H. J. Kim,¹⁵ J. H. Kim,³⁵ S. K. Kim,³⁴ P. Koppenburg,⁷ S. Korpar,^{18, 12} P. Krokovny,¹ A. Kuzmin,¹ Y.-J. Kwon,⁴⁷ S. H. Lee,³⁴ T. Lesiak,²⁵ J. Li,³³ S.-W. Lin,²⁴ J. MacNaughton,¹⁰ G. Majumder,³⁷ F. Mandl,¹⁰ T. Matsumoto,⁴³ A. Matyja,²⁵ Y. Mikami,⁴⁰ W. Mitaroff,¹⁰ K. Miyabayashi,²¹ H. Miyata,²⁷ R. Mizuk,¹¹ T. Mori,⁴² T. Nagamine,⁴⁰ Y. Nagasaka,⁸ T. Nakadaira,⁴¹ M. Nakao,⁷ S. Nishida,⁷ O. Nitoh,⁴⁴ S. Ogawa,³⁸ T. Ohshima,²⁰ T. Okabe,²⁰ S. Okuno,¹³ S. L. Olsen,⁶ W. Ostrowicz,²⁵ H. Ozaki,⁷ P. Pakhlov,¹¹ N. Parslow,³⁶ L. E. Piilonen,⁴⁶ H. Sagawa,⁷ S. Saitoh,⁷ Y. Sakai,⁷ N. Sato,²⁰ O. Schneider,¹⁶ J. Schümann,²⁴ S. Semenov,¹¹ K. Senyo,²⁰ M. E. Sevior,¹⁹ H. Shibuya,³⁸ V. Sidorov,¹ N. Soni,³⁰ R. Stamen,⁷ S. Stanič,^{45, †} M. Starič,¹² K. Sumisawa,²⁹ T. Sumiyoshi,⁴³ O. Tajima,⁴⁰ F. Takasaki,⁷ K. Tamai,⁷ N. Tamura,²⁷ M. Tanaka,⁷ G. N. Taylor,¹⁹ Y. Teramoto,²⁸ S. N. Tovey,¹⁹ T. Tsuboyama,⁷ S. Uehara,⁷ T. Uglov,¹¹ K. Ueno,²⁴ Y. Unno,² S. Uno,⁷ G. Varner,⁶ K. E. Varvell,³⁶ C. H. Wang,²³ M. Watanabe,²⁷ B. D. Yabsley,⁴⁶ Y. Yamada,⁷ A. Yamaguchi,⁴⁰ Y. Yamashita,²⁶ M. Yamauchi,⁷ J. Ying,³¹ Y. Yuan,⁹ Y. Yusa,⁴⁰ S. L. Zang,⁹ C. C. Zhang,⁹ J. Zhang,⁷ Z. P. Zhang,³³ T. Ziegler,³² and D. Žontar^{17, 12}

(The Belle Collaboration)

¹*Budker Institute of Nuclear Physics, Novosibirsk*

²*Chiba University, Chiba*

³*Chonnam National University, Kwangju*

⁴*University of Cincinnati, Cincinnati, Ohio 45221*

⁵*Gyeongsang National University, Chinju*

⁶*University of Hawaii, Honolulu, Hawaii 96822*

⁷*High Energy Accelerator Research Organization (KEK), Tsukuba*

⁸*Hiroshima Institute of Technology, Hiroshima*

⁹*Institute of High Energy Physics, Chinese Academy of Sciences, Beijing*

¹⁰*Institute of High Energy Physics, Vienna*
¹¹*Institute for Theoretical and Experimental Physics, Moscow*
¹²*J. Stefan Institute, Ljubljana*
¹³*Kanagawa University, Yokohama*
¹⁴*Korea University, Seoul*
¹⁵*Kyungpook National University, Taegu*
¹⁶*Swiss Federal Institute of Technology of Lausanne, EPFL, Lausanne*
¹⁷*University of Ljubljana, Ljubljana*
¹⁸*University of Maribor, Maribor*
¹⁹*University of Melbourne, Victoria*
²⁰*Nagoya University, Nagoya*
²¹*Nara Women's University, Nara*
²²*National Kaohsiung Normal University, Kaohsiung*
²³*National United University, Miao Li*
²⁴*Department of Physics, National Taiwan University, Taipei*
²⁵*H. Niewodniczanski Institute of Nuclear Physics, Krakow*
²⁶*Nihon Dental College, Niigata*
²⁷*Niigata University, Niigata*
²⁸*Osaka City University, Osaka*
²⁹*Osaka University, Osaka*
³⁰*Panjab University, Chandigarh*
³¹*Peking University, Beijing*
³²*Princeton University, Princeton, New Jersey 08545*
³³*University of Science and Technology of China, Hefei*
³⁴*Seoul National University, Seoul*
³⁵*Sungkyunkwan University, Suwon*
³⁶*University of Sydney, Sydney NSW*
³⁷*Tata Institute of Fundamental Research, Bombay*
³⁸*Toho University, Funabashi*
³⁹*Tohoku Gakuin University, Tagajo*
⁴⁰*Tohoku University, Sendai*
⁴¹*Department of Physics, University of Tokyo, Tokyo*
⁴²*Tokyo Institute of Technology, Tokyo*
⁴³*Tokyo Metropolitan University, Tokyo*
⁴⁴*Tokyo University of Agriculture and Technology, Tokyo*
⁴⁵*University of Tsukuba, Tsukuba*
⁴⁶*Virginia Polytechnic Institute and State University, Blacksburg, Virginia 24061*
⁴⁷*Yonsei University, Seoul*

Abstract

We report the first observation of the charmless hyperonic B decay, $B^+ \rightarrow \Lambda \bar{\Lambda} K^+$, using a 140 fb^{-1} data sample recorded at the $\Upsilon(4\text{S})$ resonance with the Belle detector at the KEKB e^+e^- collider. The measured branching fraction is $\mathcal{B}(B^+ \rightarrow \Lambda \bar{\Lambda} K^+) = (2.91^{+0.90}_{-0.70} \pm 0.38) \times 10^{-6}$. We also perform a search for the related decay mode $B^+ \rightarrow \Lambda \bar{\Lambda} \pi^+$, but do not find a significant signal. We set a 90% confidence-level upper limit of $\mathcal{B}(B^+ \rightarrow \Lambda \bar{\Lambda} \pi^+) < 2.8 \times 10^{-6}$.

PACS numbers: 13.25.Hw, 13.60.Rj

Charmless hadronic B decays are of great interest since they provide opportunities for probing CP violation, as well as for testing our understanding of strong interactions. While charmless mesonic modes were first established over ten years ago [1], B decays to charmless baryonic final states such as $p\bar{p}K^+$ [2], $p\bar{\Lambda}\pi^-$ [3], $p\bar{p}K^0$, $p\bar{p}\pi^+$ and $p\bar{p}K^{*+}$ [4] were first seen only recently. The branching ratios for these three-body decays are larger than those for two-body modes such as $B^0 \rightarrow p\bar{p}$, for which only upper limits have been reported [5]. Another intriguing feature is the threshold peaking behavior commonly observed in the baryon pair mass spectrum [2, 3, 4]. Both features were anticipated by theory [6], but the underlying dynamics are still far from understood [7, 8, 9, 10, 11, 12].

In this paper we report the observation of $B^+ \rightarrow \Lambda\bar{\Lambda}K^+$ decay, the first example of a charmless B decay to a final state containing two hyperons [13]. The rate is found to be comparable to that of other charmless three-body baryonic modes as well as that for $B \rightarrow \phi\phi K$ [14]. The invariant mass of the $\Lambda\bar{\Lambda}$ system has a prominent near-threshold peak.

With three strange particles in the final state, the $\Lambda\bar{\Lambda}K^+$ mode may complement $b \rightarrow s\bar{s}s$ dominated mesonic modes such as $B \rightarrow \phi K^{(*)}$ [15, 16, 17, 18], for which the polarization and CP asymmetry may be sensitive to new physics. With the three-body final state and self-analyzed polarization information from the Λ decay [6, 9, 10, 11], the $B^+ \rightarrow \Lambda\bar{\Lambda}K^+$ process can be used to probe not only CP violation, but T (time reversal symmetry) violation as well.

We use a data sample of 140 fb^{-1} integrated luminosity, consisting of 152 million $B\bar{B}$ pairs with no accompanying particles, collected by the Belle detector at the KEKB asymmetric energy e^+e^- (3.5 on 8 GeV) collider[19]. The Belle detector is a large solid angle magnetic spectrometer that consists of a three-layer silicon vertex detector (SVD), a 50-layer central drift chamber (CDC), an array of aerogel threshold Čerenkov counters (ACC), a barrel-like arrangement of time-of-flight scintillation counters (TOF), and an electromagnetic calorimeter comprised of CsI(Tl) crystals located inside a super-conducting solenoid coil that provides a 1.5 T magnetic field. An iron flux-return located outside of the coil is instrumented to detect K_L^0 mesons and to identify muons. The detector is described in detail elsewhere [20].

Since KEKB operates with a center-of-mass energy at the $\Upsilon(4S)$ resonance, which decays into a $B\bar{B}$ pair, one can use the following two kinematic variables to identify the reconstructed B meson candidates: the beam constrained mass, $M_{bc} = \sqrt{E_{\text{beam}}^2 - p_B^2}$, and the energy difference, $\Delta E = E_B - E_{\text{beam}}$, where E_{beam} , p_B , and E_B are the beam energy, the momentum, and energy of the reconstructed B meson in the $\Upsilon(4S)$ rest frame, respectively. The M_{bc} resolution of about $3 \text{ MeV}/c^2$ is dominated by the beam energy spread. The ΔE resolution for $B^+ \rightarrow \Lambda\bar{\Lambda}K^+$ ranges from 12 MeV to 17 MeV, depending on $M_{\Lambda\bar{\Lambda}}$.

The event selection criteria are based on the information obtained from the tracking system (SVD+CDC) and the hadron identification system (CDC+ACC+TOF), and are optimized using Monte Carlo (MC) simulated event samples.

All primary charged tracks are required to satisfy track quality criteria based on the track impact parameters relative to the interaction point (IP). The deviations from the IP position are required to be within $\pm 0.3 \text{ cm}$ in the transverse (x - y) plane, and within $\pm 3 \text{ cm}$ in the z direction, where the z axis is the opposite of the positron beam direction.

Primary kaon and pion candidates are selected based on K/π likelihood functions obtained from the hadron identification system. To identify kaons/pions, we require the likelihood ratio $L_{K(\pi)}/(L_K + L_\pi)$ to be greater than 0.6. For kaons(pions), this requirement has an efficiency of 86%(89%) and a pion(kaon) misidentification probability of 8%(10%).

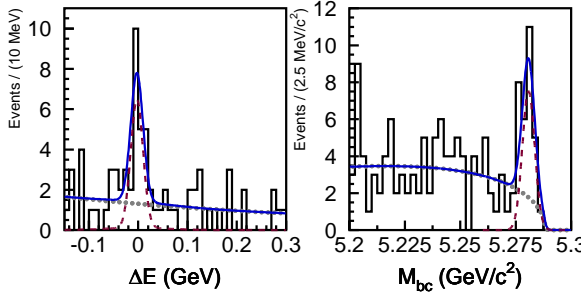


FIG. 1: ΔE and M_{bc} distributions of $B^+ \rightarrow \Lambda\bar{\Lambda}K^+$ candidates for $M_{\Lambda\bar{\Lambda}} < 2.85 \text{ GeV}/c^2$. The solid and dashed curves represent the fit results and the signal, respectively; the dotted curve shows the background contribution.

Λ candidates are reconstructed via the $p\pi^-$ decay channel using the method described in ref. [5].

The dominant background for the rare decay modes reported here is from $e^+e^- \rightarrow q\bar{q}$ continuum processes (where $q = u, d, s, c$). The background from generic B decays and known baryonic B decays is negligible. This is confirmed using an off-resonance data set (10 fb^{-1}) taken 60 MeV below the $\Upsilon(4S)$ and MC samples of generic B decay, 150 million continuum events and known baryonic B decays. In the $\Upsilon(4S)$ rest frame, continuum events tend to be jet-like while $B\bar{B}$ events tend to be spherical. We follow the scheme defined in [21] that combines 7 shape variables to form a Fisher discriminant [22] in order to optimize continuum background suppression. The variables used have almost no correlation with M_{bc} and ΔE . Probability density functions (PDFs) for the Fisher discriminant and the cosine of the angle between the B flight direction and the beam direction in the $\Upsilon(4S)$ frame are combined to form the signal (background) likelihood $\mathcal{L}_{s(b)}$. We require the likelihood ratio $\mathcal{R} = \mathcal{L}_s/(\mathcal{L}_s + \mathcal{L}_b)$ to be greater than 0.4; this suppresses about 73% of the background while retaining 88% of the signal. The selection point is determined by optimizing $S/\sqrt{S+B}$, where s and b denote the number of signal and background; here a signal branching fraction of 4×10^{-6} is assumed. We also require only one candidate per event. In the case of multiple B candidates (about 2.6% of the events), we choose the candidate with the highest \mathcal{R} value. The signal PDFs are determined using the signal MC simulation; the background PDFs are obtained from the data sideband events with $5.2 \text{ GeV}/c^2 < M_{bc} < 5.26 \text{ GeV}/c^2$ and $0.1 \text{ GeV} < |\Delta E| < 0.3 \text{ GeV}$.

To ensure the decay is charmless, we exclude $2.85 \text{ GeV}/c^2 < M_{\Lambda\bar{\Lambda}} < 3.128 \text{ GeV}/c^2$ and $3.315 \text{ GeV}/c^2 < M_{\Lambda\bar{\Lambda}} < 3.735 \text{ GeV}/c^2$ regions to remove contributions from J/ψ , η_c , ψ' and $\chi_{c0,1,2}$ in order to extract the three body decay branching fraction.

We perform an unbinned extended maximum likelihood fit to the events with $-0.15 \text{ GeV} < \Delta E < 0.3 \text{ GeV}$ and $M_{bc} > 5.2 \text{ GeV}/c^2$ to estimate signal yields. The extended likelihood function \mathcal{L} is

$$\mathcal{L} = e^{-(N_s + N_b)} \prod_{i=1}^N [N_s P_s(M_{bc_i}, \Delta E_i) + N_b P_b(M_{bc_i}, \Delta E_i)],$$

where $P_s(P_b)$ is the signal(background) PDF and $N_s(N_b)$ denotes the number of signal(background) candidates. The signal PDF is the product of a Gaussian function, which represents M_{bc} , and a double Gaussian for ΔE . The means and the widths of the signal

PDFs are determined by MC simulation. Differences between data and MC are corrected by the $B^- \rightarrow D^0\pi^-$ and $D^0 \rightarrow K^-\pi^+\pi^-\pi^+$ control sample.

We use the parametrization first suggested by the ARGUS collaboration [23], $f(M_{bc}) \propto M_{bc}\sqrt{1 - (M_{bc}/E_{beam})^2} \exp[-\xi(1 - (M_{bc}/E_{beam})^2)]$, to model the background M_{bc} distribution and a 2nd order polynomial for the background ΔE shape. We perform a two-dimensional unbinned fit to the ΔE - M_{bc} distribution, floating the signal and background normalizations as well as the background shape parameters.

The M_{bc} distribution (with $|\Delta E| < 0.05$ GeV) and the ΔE distribution (with $M_{bc} > 5.27$ GeV/c^2) for the region $M_{\Lambda\bar{\Lambda}} < 2.85$ GeV/c^2 (*i.e.* below charmonium threshold) are shown in Fig. 1 with fit results overlaid. The two-dimensional unbinned fit gives a signal yield of $22.9^{+5.8}_{-4.8}$ with a statistical significance of 7.4 standard deviations. The significance is defined as $\sqrt{-2\ln(L_0/L_{\max})}$, where L_0 and L_{\max} are the likelihood values returned by the fits with signal yield fixed at zero and floating, respectively [24].

We fit the signal yield in bins of $M_{\Lambda\bar{\Lambda}}$ and the result as a function of $\Lambda\bar{\Lambda}$ mass is shown in Fig. 2. The observed mass distribution peaks at low $\Lambda\bar{\Lambda}$ mass, similar to those observed in [2, 3, 4]. Since the decay is not uniform in phase space, we calculate the partial branching fraction for each $M_{\Lambda\bar{\Lambda}}$ bin with the corresponding detection efficiency determined from a large phase space MC sample and an additional special MC sample with a $M_{\Lambda\bar{\Lambda}}$ peak near threshold[25]. The $\Lambda\bar{\Lambda}$ invariant mass spectrum for the events in the $B^+ \rightarrow \Lambda\bar{\Lambda}K^+$ signal region ($|\Delta E| < 0.05$ GeV and $M_{bc} > 5.27$ GeV/c^2) with $2.85 \text{ GeV}/c^2 < M_{\Lambda\bar{\Lambda}} < 3.15 \text{ GeV}/c^2$ is shown in the inset of Fig. 2. A clear J/ψ signal is evident. The results of the fits along with the efficiencies and the partial branching fractions are given in Table I. We sum the partial branching fractions in Table I to obtain $\mathcal{B}(B^+ \rightarrow \Lambda\bar{\Lambda}K^+) = (2.91^{+0.90}_{-0.70} \text{ (stat)} \pm 0.38 \text{ (syst)}) \times 10^{-6}$, with a statistical significance of 5.1 standard deviations.

The systematic uncertainty in particle selection is studied using high statistics control samples. Kaon/pion identification is studied with a $D^{*+} \rightarrow D^0\pi^+$, $D^0 \rightarrow K^-\pi^+$ sample. The

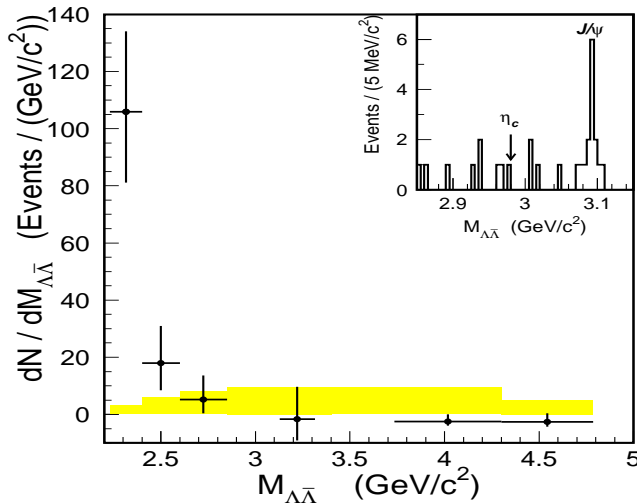


FIG. 2: Fitted yield divided by bin size for $B^+ \rightarrow \Lambda\bar{\Lambda}K^+$ as a function of $M_{\Lambda\bar{\Lambda}}$. The shaded distribution is from a phase space MC simulation with the area normalized to the signal yield. Note that the charmonium veto has been applied. The inset shows the $\Lambda\bar{\Lambda}$ mass spectrum for the η_c and J/ψ signal regions.

TABLE I: Results of the $\Delta E - M_{bc}$ fit, detection efficiencies (ϵ), and branching fractions (\mathcal{B}) with statistical errors in bins of $M_{\Lambda\bar{\Lambda}}$ after the charmonium veto has been applied. The fit allows the yields to fluctuate negative. Note that the yields are consistent with zero above charmonium threshold.

$M_{\Lambda\bar{\Lambda}}$ (GeV)	Signal Yield	Efficiency(%)	\mathcal{B} (10^{-6})
< 2.4	$18.0^{+4.8}_{-4.2}$	4.83	$2.45^{+0.65}_{-0.57}$
2.4 – 2.6	$3.6^{+2.6}_{-1.9}$	4.30	$0.55^{+0.40}_{-0.29}$
2.6 – 2.85	$1.3^{+2.1}_{-1.2}$	4.04	$0.21^{+0.34}_{-0.20}$
3.128 – 3.315	$-0.3^{+2.1}_{-1.4}$	5.19	$-0.04^{+0.27}_{-0.18}$
3.735 – 4.3	$-1.4^{+1.4}_{-0.8}$	6.60	$-0.14^{+0.14}_{-0.08}$
> 4.3	$-1.3^{+1.5}_{-0.8}$	6.90	$-0.12^{+0.14}_{-0.08}$
Total	$19.9^{+6.5}_{-5.1}$	-	$2.91^{+0.90}_{-0.70}$

tracking efficiency is studied with a D^* sample, using both full and partial reconstruction. Based on these studies, we assign a 7.8% error for the tracking efficiency and 0.6% for kaon/pion identification.

For Λ reconstruction we have an additional error on the efficiency for off-IP tracks reconstruction, determined from the difference of Λ proper time distributions for data and MC simulation. For the four tracks from the $\Lambda\bar{\Lambda}$ pair this error amounts to 6.1%. By studying the $\Lambda \rightarrow p\pi^-$ sample we assign an error of 1% for each identified proton. There is also a 1% error for each Λ mass selection and a 0.7% error for each Λ vertex selection [5]. Summing the correlated errors for Λ and $\bar{\Lambda}$ reconstruction, we obtain a systematic error of 6.9% for both Λ 's.

Continuum suppression is studied with the topologically similar $B^- \rightarrow D^0\pi^-$, $D^0 \rightarrow K^-\pi^+\pi^+\pi^-$ sample. By changing the selection criteria on \mathcal{R} in the interval 0 – 0.4, the efficiencies of data and MC differ by 3%.

The systematic uncertainty from fitting is 4.9%, which is studied by varying the parameters of the signal and background PDFs by $\pm 1\sigma$. The MC statistical uncertainty and modelling with six $M_{\Lambda\bar{\Lambda}}$ bins contributes a 5.0% error(obtained by changing the $M_{\Lambda\bar{\Lambda}}$ bin size). The error on the number of total $B\bar{B}$ pairs is determined to be 0.7%. The error from the sub-decay branching fraction of $\Lambda \rightarrow p\pi^-$ is 0.8% [24].

We sum the correlated errors linearly and then combine the result with the uncorrelated ones in quadrature. The total systematic error is 13.0%.

We perform a cross-check of this analysis by using the charmonium-veto events. We measure $\mathcal{B}(B^+ \rightarrow J/\psi K^+)$ by following the same analysis procedure with $3.06 \text{ GeV}/c^2 < M_{\Lambda\bar{\Lambda}} < 3.14 \text{ GeV}/c^2$. The signal yield is $11.4^{+3.9}_{-3.2}$ candidates with a statistical significance of 7.3 standard deviations. The obtained product branching fraction is $\mathcal{B}(B^+ \rightarrow J/\psi K^+) \times \mathcal{B}(J/\psi \rightarrow \Lambda\bar{\Lambda}) = (1.55^{+0.53}_{-0.44}) \times 10^{-6}$. By using $\mathcal{B}(B^+ \rightarrow J/\psi K^+) = (1.01 \pm 0.05) \times 10^{-3}$ [24], our measured branching fraction is $\mathcal{B}(J/\psi \rightarrow \Lambda\bar{\Lambda}) = (1.54^{+0.53}_{-0.43} \pm 0.20 \pm 0.08) \times 10^{-3}$, which is in agreement with the world average[24]. The third error comes from the uncertainty of $\mathcal{B}(B^+ \rightarrow J/\psi K^+)$.

We also search for the decay mode $B^+ \rightarrow \Lambda\bar{\Lambda}\pi^+$, which is an example of a $b \rightarrow u\bar{u}d$ process with $s\bar{s}$ popping. The background from $B^+ \rightarrow \Lambda\bar{\Lambda}K^+$ is negligible. We perform a

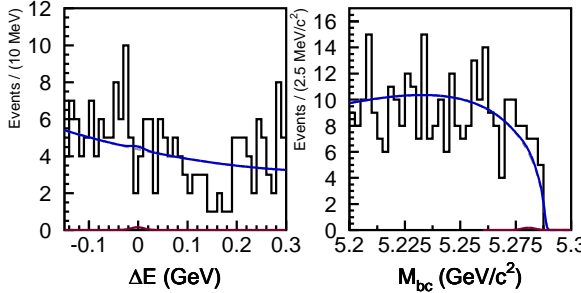


FIG. 3: ΔE and M_{bc} distributions for $B^+ \rightarrow \Lambda\bar{\Lambda}\pi^+$ candidates. The solid curve is the fit result.

two-dimensional unbinned likelihood fit to the ΔE - M_{bc} distribution using the same analysis procedure. No significant signal is found. The M_{bc} and ΔE distributions with fit projections are shown in Fig.3. We use the fit results to estimate the expected background, and compare this with the observed number of events in the signal region in order to set an upper limit on the yield at the 90% confidence level [26]. The estimated background is 37.5 ± 1.0 , the number of observed events is 41, the systematic uncertainty is 15%, and the upper limit yield is 21.7. The efficiency, estimated from the phase space MC, is found to be 5.05%. The 90% confidence level upper limit for the branching fraction is $\mathcal{B}(B^+ \rightarrow \Lambda\bar{\Lambda}\pi^+) < 2.8 \times 10^{-6}$.

In summary, we have performed a search for the rare baryonic decays $B^+ \rightarrow \Lambda\bar{\Lambda}K^+$ and $\Lambda\bar{\Lambda}\pi^+$ with 152 million $B\bar{B}$ events. A clear signal is seen in the $B^+ \rightarrow \Lambda\bar{\Lambda}K^+$ mode, where we measure a branching fraction of $\mathcal{B}(B^+ \rightarrow \Lambda\bar{\Lambda}K^+) = (2.91^{+0.90}_{-0.70} \pm 0.38) \times 10^{-6}$, which is comparable to $B^+ \rightarrow p\bar{p}K^+$ and $B^0 \rightarrow p\bar{\Lambda}\pi^-$. The observed $M_{\Lambda\bar{\Lambda}}$ spectrum peaks toward the threshold as in the above mentioned modes. This measurement is the first observation of a B meson decay to a hyperon pair through a $b \rightarrow s\bar{s}s$ process. The $B^+ \rightarrow \Lambda\bar{\Lambda}\pi^+$ mode is not statistically significant, and we set the 90% confidence level upper limit $\mathcal{B}(B^+ \rightarrow \Lambda\bar{\Lambda}\pi^+) < 2.8 \times 10^{-6}$.

We thank the KEKB group for the excellent operation of the accelerator, the KEK Cryogenics group for the efficient operation of the solenoid, and the KEK computer group and the NII for valuable computing and Super-SINET network support. We acknowledge support from MEXT and JSPS (Japan); ARC and DEST (Australia); NSFC (contract No. 10175071, China); DST (India); the BK21 program of MOEHRD and the CHEP SRC program of KOSEF (Korea); KBN (contract No. 2P03B 01324, Poland); MIST (Russia); MESS (Slovenia); NSC and MOE (Taiwan); and DOE (USA).

* on leave from Fermi National Accelerator Laboratory, Batavia, Illinois 60510

† on leave from Nova Gorica Polytechnic, Nova Gorica

- [1] M. Battle *et al.* (CLEO Collaboration), Phys. Rev. Lett. **71**, 3922 (1993).
- [2] K. Abe *et al.* (Belle Collaboration), Phys. Rev. Lett. **88**, 181803 (2002).
- [3] M.-Z. Wang *et al.* (Belle Collaboration), Phys. Rev. Lett. **90**, 201802 (2003).
- [4] M.-Z. Wang *et al.* (Belle Collaboration), Phys. Rev. Lett. **92**, 131801 (2004).
- [5] K. Abe *et al.* (Belle Collaboration), Phys. Rev. D **65**, 091103 (2002); B. Aubert *et al.* (BaBar

Collaboration), Phys. Rev. D **69**, 091503 (2004).

[6] W.S. Hou and A. Soni, Phys. Rev. Lett. **86**, 4247 (2001); C.K. Chua, W.S. Hou and S.Y. Tsai, Phys. Lett. **B528**, 233 (2002).

[7] F. Piccinini and A.D. Polosa, Phys. Rev. D **65**, 097508 (2002); H.Y. Cheng and K.C. Yang, Phys. Lett. **B533**, 271 (2002).

[8] H.Y. Cheng and K.C. Yang, Phys. Rev. D **66**, 014020 (2002).

[9] C.K. Chua, W.S. Hou and S.Y. Tsai, Phys. Rev. D **66**, 054004 (2002).

[10] M. Suzuki, J. Phys. G **29**, B15 (2003).

[11] C. K. Chua and W. S. Hou, Eur. Phys. J. C **29**, 27 (2003).

[12] J. L. Rosner, Phys. Rev. D **68**, 014004 (2003).

[13] Throughout this report, the inclusion of charge conjugate mode is always implied unless otherwise stated.

[14] H.-C. Huang *et al.* (Belle Collaboration), Phys. Rev. Lett. **91**, 241802 (2003).

[15] K.-F. Chen, A. Bozek, *et al.* (Belle Collaboration), Phys. Rev. Lett. **91**, 201801 (2003).

[16] K. Abe *et al.* (Belle Collaboration), Phys. Rev. Lett. **91**, 261602 (2003).

[17] B. Aubert *et al.* (BaBar Collaboration), Phys. Rev. Lett. **91**, 171802 (2003).

[18] B. Aubert *et al.* (BaBar Collaboration), arXiv:hep-ex/0403026.

[19] S. Kurokawa and E.Kikutani, Nucl. Instrum. Meth. A **499**, 1 (2003), and other papers included in this volume.

[20] A. Abashian *et al.* (Belle Collaboration), Nucl. Instr. and Meth. A **479**, 117 (2002).

[21] K. Abe *et al.* (Belle Collaboration), Phys. Lett. **B517**, 309 (2001).

[22] R.A. Fisher, Annals of Eugenics **7**, 179 (1936).

[23] H. Albrecht *et al.* (ARGUS Collaboration), Phys. Lett. B **229**, 304 (1989).

[24] K. Hagiwara *et al.* (Particle Data Group), Phys. Rev. D **66**, 010001 (2002).

[25] We generated a special $B^+ \rightarrow \Lambda\bar{\Lambda}K^+$ MC sample with $2.23 \text{ GeV}/c^2 < M_{\Lambda\bar{\Lambda}} < 2.85 \text{ GeV}/c^2$. The efficiency was obtained using 1.6×10^5 events generated according to phase space and 5×10^4 events of special MC.

[26] G.J. Feldman and R.D. Cousins, Phys. Rev. D **57**, 3873 (1998); J. Conrad, O. Botner, A. Hallgren and Perez de los Heros, C. Phys. Rev. D **67**, 012002 (2003).